Electrostatic Properties of Cytochrome *f*: Implications for Docking with Plastocyanin

Douglas C. Pearson, Jr., Elizabeth L. Gross, and Erico S. David
Department of Biochemistry and Biophysics Program, The Ohio State University, Columbus, Ohio 43210 USA

ABSTRACT The electrostatic properties of cytochrome *f* (cyt *f*), a member of the cytochrome b_6f complex and reaction partner with plastocyanin (PC) in photosynthetic electron transport, are qualitatively studied with the goal of determining the mechanism of electron transfer between cyt *f* and PC. A crystal structure for cyt *f* was analyzed with the software package GRASP, revealing a large region of positive potential generated by a patch of positively charged residues (including K58, K65, K66, K122, K185, K187, and R209) and reinforced by the iron center of the heme. This positive field attracts the negative charges of the two acidic patches on the mobile electron carrier PC. Three docked complexes are obtained for the two proteins, based on electrostatic or hydrophobic interactions or both and on steric fits by manual docking methods. The first of these three complexes shows strong electrostatic interactions between K187 on cyt *f* and D44 on PC and between E59 on PC and K58 on cyt *f*. Two other manually docked complexes are proposed, implicating H87 on PC as the electron-accepting site from the iron center of cyt *f* through Y1. The second complex maintains the D44/K187 cross-link (but not the E59/K58 link) while increasing hydrophobic interactions between PC and cyt *f*. Hydrophobic interactions are increased still further in the third complex, whereas the link between K187 on cyt *f* and D44 on PC is broken. The proposed reaction mechanism, therefore, involves an initial electrostatic docking complex that gives rise to a nonpolar attraction between the regions surrounding H87 on PC and Y1 on cyt *f*, providing for an electron-transfer active complex.

INTRODUCTION

Plastocyanin (PC) and cytochrome *f* (cyt *f*) are reaction partners in the photosynthetic electron transport chain. PC is a mobile electron carrier in the lumen of the thylakoid, and cyt *f* is a member of the cytochrome b_6f complex, which is bound to the thylakoid membrane. PC receives an electron from cyt *f* and shuttles it to the P700 reaction center of the photosystem I complex (Gross, 1996). The specific mechanism for the electron transfer reaction between PC and cyt *f* has not been elucidated.

PC, shown in Fig. 1 *A*, is a "blue" copper protein of ~10 kDa, closely related to other copper proteins such as azurin and stellacyanin (Freeman, 1981). Its structure is that of a Greek key β-barrel, with a copper center coordinated to four ligands—two histidine residues (H37, H87), a cysteine residue (C84), and a methionine residue (M92)—in a distorted tetrahedral geometry (Gross, 1996). Several three-dimensional structures of PC have been determined, including the x-ray crystallography structure for poplar PC in oxidized (Guss and Freeman, 1983) and reduced (Guss et al., 1992) forms and the NMR structure for reduced parsley PC (Bagby et al., 1994). Important features of poplar PC include the surface-exposed H87, Y83, and two patches of negatively charged residues: Patch 1, #42–44 and #79; Patch 2: #59–61. In spinach and french bean PC, the fourth charge in Patch 1 is residue #45 rather than #79 (Gross, 1996). (For other reviews on PC, see Gross (1993) and Sykes (1991).)

Cyt *f*, displayed in Fig. 1 *B*, is the largest of the known members of the cytochrome b_6f complex, with an molecular weight of ~31,000. The crystal structure of the soluble domain of turnip cyt *f* (~27 kDa, 252 of 285 residues plus heme) was recently determined by Martinez and co-workers (1995b). It is organized into two β-sheet folding domains, a small domain of 63 residues and a large heme-binding domain of 189 residues. It has the usual *c*-type cytochrome heme ligation with one notable exception: The distal iron ligand is the amino group of the N-terminal tyrosine residue, which is unprecedented for any heme protein (Martinez et al., 1995b). Y1 is positioned on the surface of cyt *f*, covering the heme. The only portions of the heme that are exposed to the surface are the two propionic acid side chains. R156, which is located adjacent to the propionic acid side chains on the heme, partially balances their negative charges. Also of note are a series of positively charged residues including K58, K65, K66, K122, K185, K187, and R209. All these except R209 are conserved in cyt *f* from higher plants and green algae.

A recent refinement of the cyt *f* structure reveals the presence of an internal water chain entering the protein within 6 Å of lysine-66 on the protein surface and ending within hydrogen bond distance of the iron center. The possible role of this water chain in hydrogen ion translocation or in electron transfer is still a matter of debate (Martinez et al., 1995b).

From NMR studies of PC, two potential binding sites for redox partners have been inferred (Cookson et al., 1980; Handford et al., 1980), as shown in Fig. 1 *A*. Site 1 involves the region around H87, largely a region of positive potential

Received for publication 10 August 1996 and in final form 15 March 1996
Address reprint requests to Dr. Elizabeth L. Gross, Department of Biochemistry, The Ohio State University, 484 West 12th Avenue, Columbus, OH 43210. Tel.: (614) 292-9480, Fax: (614) 292-6773, E-mail: egross@magnus.acs.ohio-state.edu.

0006-3495/96/07/64/13 $2.00

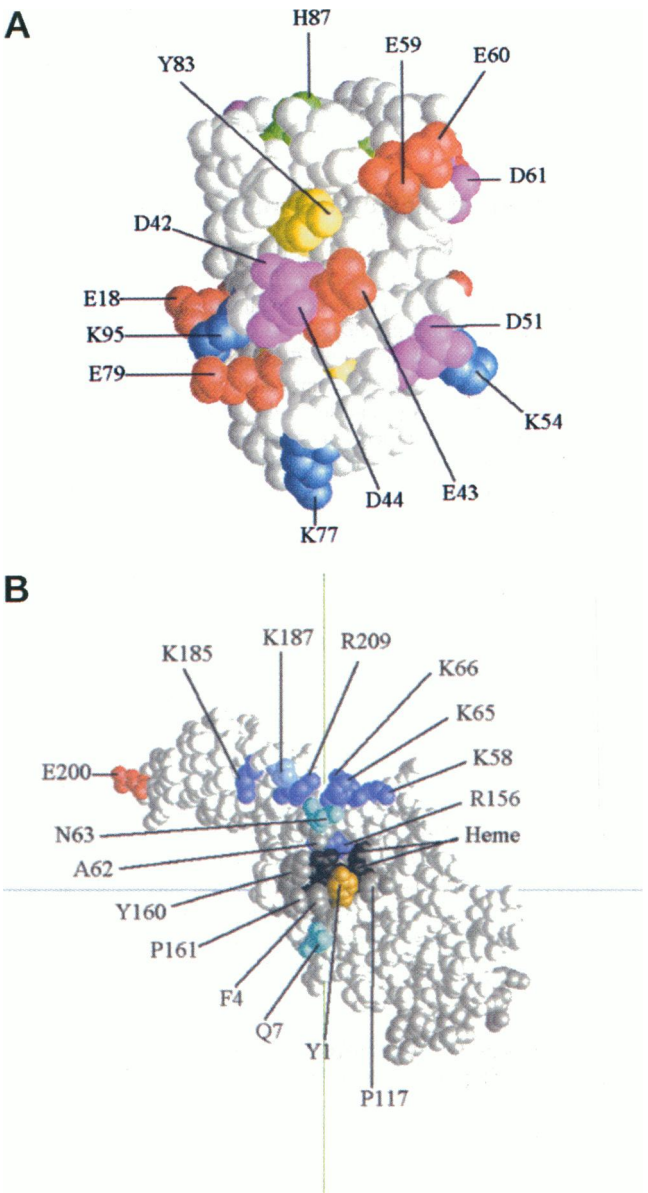

FIGURE 1 Molecular graphic representations of poplar PC (*A*; Guss et al., 1992) and turnip cyt *f* (*B*; Martinez et al., 1995a,b) as prepared by GRASP (Nicholls et al., 1991) for Silicon Graphics IRIS workstations. Key residues of interest in this work are labeled. (*A*) Colors are assigned to residues as follows: Y83, yellow; H87, green; key aspartates, magenta; key glutamates, red; key lysines, blue. (*B*) Colors are assigned to residues as follows: Y1, yellow; heme, black; K187, light blue; all positively charged residues except K187, dark blue; E200, red; key polar residues, cyan; key nonpolar residues, gray.

very close to the copper center, also surrounded by several hydrophobic residues. Electron transfer at Site 1 involves an outer sphere mechanism through the H87 ligand to the copper atom. Site 2 involves the region around tyrosine-83, which has a through bond pathway to cysteine-84 (C84), which is a ligand to the copper. The Site 2 region includes two patches of acidic residues, residues 42–44 and residues 59–61. Because of this, Y83 is at the center of a large region of negative potential (Durell et al., 1990). Fig. 1 *A* also points out other key residues of interest on PC.

Several pieces of evidence have implicated Site 2 in the interaction of PC with cyt *f*. Chemical cross-linking studies have pinpointed two links: between aspartate-44 on PC and lysine-187 on cyt *f*, and between glutamate-59 or glutamate-60 on PC and an unidentified residue on cyt *f* (Morand et al., 1989). Evidence from Qin and Kostic (1993) suggests that the cross-linked derivatives are inactive with regard to intermolecular electron transfer; however, other evidence (Takabe and Ishikawa, 1989; D.J. Davis, unpublished results) would suggest that this question is still open. Chemical modification of acidic residues of spinach on PC in either the 42–45 cluster or the 59–61 cluster (Anderson et al., 1987) severely inhibited the interaction of PC with cyt *f*. Site-directed mutagenesis studies on Y83 suggest that, as long as an aromatic residue is located at position 83, electron transfer can take place; however, the bimolecular binding constant for a Y83F mutant is decreased (Modi et al., 1992a).

Evidence against Site 2 as the site for this interaction includes the following results. Mutagenesis of aspartate-42 appears to have no effect on electron transfer between PC and cyt *f* (Modi et al., 1992b). Mutagenesis of leucine-12, in the region of Site 1 (Fig. 1 *A*) revealed a decrease in binding to cyt *f* for L12E and L12A mutants but an increase in binding for an L12N mutant, implying a possible hydrogen bond between the mutated asparagine and a residue on cyt *f* (Modi et al., 1992b).

It is widely asserted that electrostatic interactions play a major role in the association of macromolecules, especially proteins (Durell et al., 1990; Northrup et al., 1988; Matthew, 1985; Harvey, 1989; Sharp and Honig, 1990; Davis et al., 1991; Warshel and Aqvist, 1991; Watkins et al., 1994). These interactions can be divided into two categories. Long-range interactions, which tend to be monopole–monopole or dipole–dopole in nature, influence the rate of association between two molecules. Short-range interactions, which tend to be far more complex, influence the alignment and orientation of the two molecules around the docking site. Long-range interactions are due for the most part to the net charge of the molecules, whereas short-range interactions are very sensitive to the distribution of charges about the molecules (Durell et al., 1990). The major goal of this research is to study qualitatively the electrostatic interactions between PC and cyt *f* and to make determinations of potential docks between PC and cyt *f* by generating docks that explain experimental results and are also electrostatically favorable. Durell and co-workers (1990) studied the electrostatic potential field of PC in some detail; however, the elucidation of the crystal structure of the soluble domain of cyt *f* (Martinez et al., 1995a,b) is recent enough that a separate analysis of its electrostatic properties is necessary here before we can begin to discuss the docking of PC with cyt *f*.

There are two dominant philosophies for calculating electrostatic properties of proteins. An excellent review of this

topic has been written by Harvey (1989). The model of Sharp and Honig (1990) is a continuum model, involving assigning dielectric constants to the volumes inside and outside the protein's surface and solving the classical Poisson–Boltzmann electrostatic equation for the charges on that protein. The methods used in the programs DelPhi (Sharp and Honig, 1990; Nicholls and Sharp, 1989) and GRASP (Nicholls et al., 1991) reflect this thinking. Practically, this works well for most problems; however, this method has two properties that may be troublesome for the pure theorist. First, and most fundamentally, it is difficult to say that the interior of a macromolecule has a dielectric constant at all, in the purest sense of the term. The dielectric constant is a macroscopic property, and the electrostatic properties of a macromolecule are by their very nature microscopic (Harvey, 1989). Second, a model that treats the solution exterior to a macromolecule as a dielectric material is by its very nature a static model. Should a significant conformational change or motion of internal water molecules be a determining factor of a macromolecule's function, a static model is inadequate to describe that function (Yelle et al., 1995). The protein dipoles–Langevin dipoles model of Warshel and Aqvist (1991) addresses both of these concerns by treating each atom explicitly in terms of polarizations; polarization is a microscopic property, and the treatment of each individual atom lends itself to dynamic treatments more than the continuum model does. We use the continuum model in these studies for two primary reasons: one, the software to solve the Poisson–Boltzmann equation for macromolecules (specifically GRASP, for purposes of this research) is readily available; two, we have no reason to believe at this time that significant conformational changes or motion of internal water molecules have a role in the function of PC or cyt *f*. The results of Martinez et al. (1995a) detecting the presence of the water chain in cyt *f* should be noted and remembered, though; although a future observation that the water chain does have a role in the function of cyt *f* will not nullify these results, it will suggest a need for a dynamic analysis of the electrostatics of PC and cyt *f*.

METHODS

Atomic coordinates

The atomic coordinates of oxidized poplar (Guss et al., 1992) PC were obtained from the Brookhaven Protein Data Bank (Bernstein et al., 1977). The atomic coordinates of reduced cyt *f* were obtained from Martinez (Martinez et al., 1995a,b).

Calculation of electrostatic potential fields

All electrostatic potential fields were calculated with the computer program GRASP (Nicholls et al., 1991), written and distributed by Anthony Nicholls of Columbia University for use on Silicon Graphics workstations running IRIX 4.0 and above; we used IRIS Indigo workstations for this work. This program utilizes a double-grid variation of the finite-difference Poisson–Boltzmann method of Sharp and Honig (1990) to solve electrostatic potential for a collection of charges, using a macroscopic approach. Charges are mapped onto two grids: a small 33 × 33 × 33 grid just enveloping the protein and a second 33 × 33 × 33 grid with twice the spacing. This method is similar, but not identical, to the method used by the DelPhi package of Sharp and Nicholls (1989). The molecular surface is defined by use of the van der Waals radii of each atom (except hydrogens).

Assignment of dielectric constants and charges

The dielectric constants inside and outside the protein surface were set to 2 and 80, respectively. For analysis at pH 7, the charge of each oxygen on an acidic residue (aspartate, glutamate, and the porphyrin carboxyls on cyt *f*) was set to $-0.5e$, and the charge of each nitrogen on a basic residue (lysine, arginine) was set to $+1.0e$. The iron atom in cyt *f* was given charges of +2 and +3 and the copper atom in plastocyanin was given charges of +2 and +1 to simulate conditions before and after electron transfer, respectively. The charge on the sulfur atom on C84 of plastocyanin was set to −1.0. Both of the histidine residues (H87 and H37) are ligands to the copper and would not be protonated at pH values of ≥5 for oxidized PC. Likewise, the amino group on Y1 of cyt *f* is never protonated because it is the sixth ligand to the heme. H25 on cyt *f* is also a ligand to the heme and, thus, cannot be protonated. An average electrostatic map calculation on GRASP took 20–30 s.

pKs and charges on titratable residues were calculated by use of the program Macrodox (Northrup, 1995) by the method of Matthew and Gurd (1986). This method confirmed the charge assignments for pH 7 listed above with the addition that the α-amino group on I1 of PC should also have a charge of +1. However, the protonation state of the amino groups on I1 has a negligible effect on the electrostatic field of PC and its ability to dock with cyt *f* (data not shown), which confirms the results of earlier chemical modification studies of amino groups on PC (Gross et al., 1990). H142, the only other histidine (besides H25), is predicted to be protonated at pH 5 but not at pH 7 but has little effect on the electrostatic field of cyt *f* because of its location on the side of the molecule opposite the heme and the conserved positive charges. We used pK values of ionizable residues calculated by Macrodox to determine the charges on cyt *f* at pH 5. These charges were then transferred to GRASP for electrostatic field calculations.

Calculations of potentials at specific points surrounding the cyt *f* molecule

Coordinates for five points on a semicircular arc 50 Å away from the iron center of cytochrome *f* and approximately perpendicular to the molecule were established for the purpose of measuring the potential at key, explicit points around the protein. We used these points to study potential as a function of ionic strength and to determine the effect of eliminating key charged residues. Whenever necessary, potentials from the binary map generated by GRASP were mapped to an ASCII file in PDB format by a program entitled PHITOPDB within the DelPhi package.

Docking configurations

Docking configurations were created and other simple molecular manipulations were performed with the HyperChem molecular modeling package distributed by AutoDesk. Whenever "manual docking" was carried out, the biochemical and biophysical criteria for establishing the dock were always related to available experimental data, as will be discussed below. A "dock" was determined to have been established and a complex formed when key residues of interest were within 5 Å and when severe steric overlap (more than five residues within 4 Å of one another) was eliminated. Two residues on different molecules were defined as interacting when they were within 6 Å of each other; they were defined as overlapping when within 4 Å. Electrostatic fields were calculated for the docked complexes by use of the charge assignments and dielectric constant criteria described above. Although this is not shown, electrostatic fields were calculated with the proteins separated by various distances.

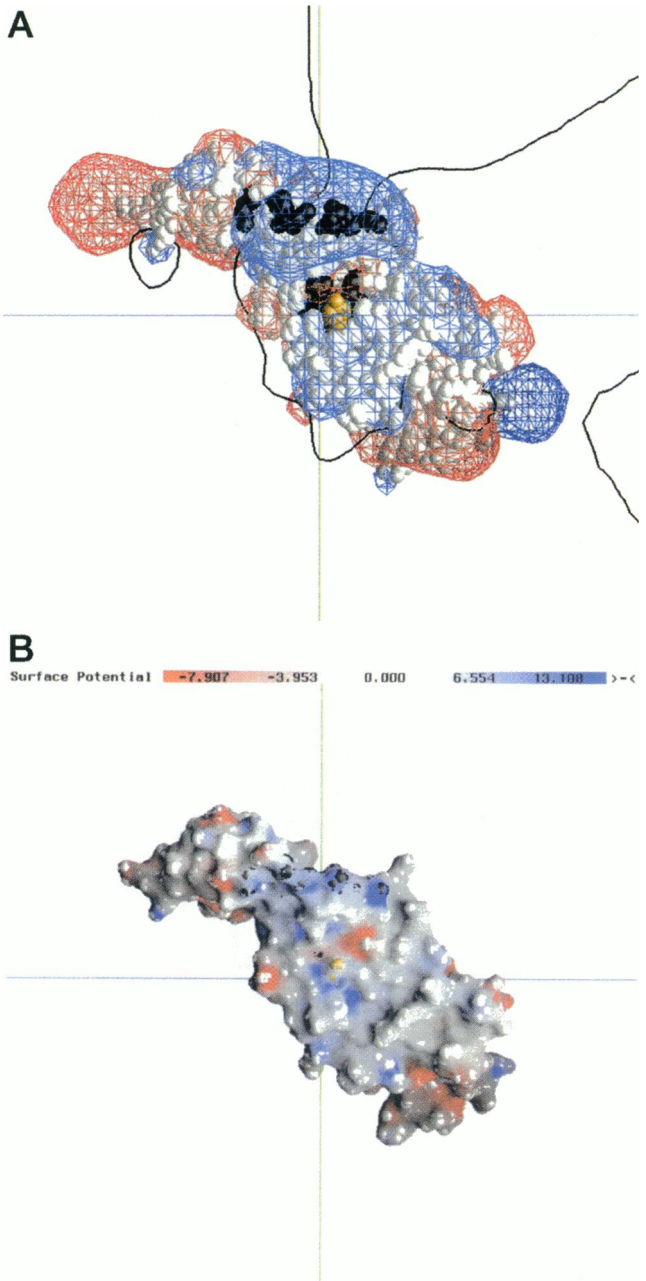

FIGURE 2 Electrostatic potential field of reduced cyt *f*. Electrostatic fields were calculated by use of the linearized Poisson–Boltzmann equation solver within the program GRASP (Nicholls et al., 1991). The ionic strength was 100 mM. (*A*) Three-dimensional electrostatic potential contours. The red contour represents a potential of −1 kT/*e*; blue, +1 kT/*e*. The black curves represent the zero (two-dimensional) contour in the plane of the figure. (*B*) Molecular surface of reduced cyt *f* as solved by GRASP. Surface potentials are colored as noted on the appropriate scale.

Hydrophobic interaction energies for Complexes 2 and 3

Hydrophobic energies were estimated based on predictions (Janin and Chothia, 1990; Rose and Wolfenden, 1993; Sharp et al., 1991) of contribution per square angstrom of covered hydrophobic surface area of 25–47 cal mol^{-1}. Hydrophobic atoms in either protein were defined as aliphatic or aromatic carbon atoms or sulfur atoms; the exposure of all atoms to the surface of the protein was calculated by a Richards surface algorithm (Lee and Richards, 1971; Richards, 1977) incorporated into the program Macrodox (Northrup, 1995). For each residue on a protein involved in a complex (as given in Tables 1–3, discussed below), surface areas were added for all surface-exposed hydrophobic atoms in that residue; the total covered surface area was considered to be twice the hydrophobic surface area on the protein that contributed *less* covered hydrophobic surface to the complex. This figure was then multiplied by 25 and 47 cal mol^{-1} to give a range of interaction energies possible.

RESULTS

Electrostatic field of cytochrome *f*

Fig. 2 *A* shows the electrostatic potential field of reduced turnip cytochrome *f* as calculated by GRASP at an ionic strength of 100 mM. The red and blue contours represent the electrostatic fields at +1 and −1 kT/*e*, respectively. The black curve represents the zero-potential contour line. It is immediately apparent that there is a large region of positive potential surrounding the center of the molecule directly over the line of positively charged residues extending from K187 to K58. This region of positive potential is also evident on the surface of the cyt *f* molecule (Fig. 2 *B*), where the contribution of the iron center of the heme to the positive potential field becomes evident.

Of special note is the disruption of the positive potential by the carboxyl groups on the propionic acid side chains on the porphyrin ring, which, in cyt *f* (unlike in mammalian cyt *c*) are exposed to the surface. Because of the surface exposure, the charges on these oxygen atoms were set to $-0.5e$. These negative charges decrease the positive potential at the surface of cyt *f* around the heme. This region of negative potential can be seen on the surface of cyt *f* (Fig. 2 *B*).

Also shown is the zero-contour line, which extends outward from the region of the positively charged residues. The field is positively charged because of the patch of positively charged residues (K58, K65, K66, K187, and R209, among others) within the two lines and can act as a beacon to attract negatively charged PC.

In addition to the large region of positive potential, there are two negatively charged regions on turnip cyt *f* at either end of the molecule. One negative patch involves D196 and E200 in the small domain. The negative patch on the small domain is diminished in cyt *f* from other species because E200 is not conserved. The other negative patch is on the large domain and involves D32, E34, E79, E95, D240, and E242, among others.

Ionic strength effects

Based on the assertion that the interaction between PC and cyt *f* is electrostatic in nature, the strength of that interaction should be sensitive to environmental factors such as pH and ionic strength as well as the oxidation states of the copper and iron centers of PC and cyt *f*, respectively. Ionic strength effects are important in light of previous studies of the interaction of PC and cyt *f* as a function of ionic strength

(Anderson et al., 1987; Takabe and Ishikawa, 1989; Qin and Kostic, 1993) and, more importantly, because the of the observation that an electrostatic (i.e., noncovalent) complex can be formed only under very low ionic strength conditions (Qin and Kostic, 1993)

Fig. 3 *A–C* displays the three-dimensional contours surrounding cyt *f* for ionic strengths of 2, 25, and 200 mM. (An ionic strength of 2 mM is used in lieu of an ionic strength of 0 for two reasons: 1) physiological: an ionic strength of 0 is unrealistically low, 2) computational: the computed electrostatic field for cyt *f* at an ionic strength of 0 varies drastically as a function of algorithm used (i.e., the double-grid algorithm of GRASP and a single grid with boundary conditions used in DelPhi). However, the results of the two algorithms agree at ionic strengths of 2 mM and above.) In an examination of the electrostatic potentials of cyt *f* as a function of ionic strength (Figs. 2 *A* and 3 *A–C*), two important effects become apparent. First, the magnitude of the positive electrostatic potential decreases with increasing ionic strength. These results alone may explain the observed decrease with increasing ionic strength of the rate of reaction of cyt *f* with both PC (Niwa et al., 1980; Takabe et al., 1986; Anderson et al., 1987; Takabe and Ishikawa, 1989) and negatively charged artificial electron transfer agents such as ferricyanide and ferrocyanide (Takabe et al., 1980). However, there is a second effect that may be important for molecules that interact directly at the heme (or Y1). At 2-mM ionic strength, the positive field is so large that it covers the vicinity of the heme, overshadowing the negative field observed in this region at 100-mM ionic strength. As the ionic strength increases, the positive field draws back from the area of the propionic acid side chains of the heme, exposing the negative field underneath it. This effect is already apparent at 25-mM ionic strength, and the exposure of the negative field becomes larger as the ionic strength is increased still further. The change in the sign of the field can be seen in Fig. 4 *D*, as will be discussed shortly.

Fig. 4 shows the magnitude of the potential as a function of location about the cyt *f* molecule. First, five points 50 Å away from the iron center of the heme were selected for computational analysis; their locations are shown in Fig. 4 *A*, where they are numbered 1–5. Then, electrostatic fields about cyt *f* were calculated for several ionic strengths between 0 and 100 mM, and the potential was mapped onto those points. Fig. 4 *B* shows a plot of potential against ionic strength at each of those five points. These results confirm that both the positive and negative fields decrease with increasing ionic strength and that the positive field is strongest at point 4, where the influence of the patch of positively charged residues is the greatest.

Second, we wished to determine how far from the molecular surface the positive field extends. To do this, we established an axis of points running from the iron atom to point 4 at a spacing of 2.5 Å apart. Electrostatic potentials were mapped onto these points and plotted as a function of distance for five different ionic strengths, as shown in Fig. 4 *C*. (Distances on the *x* axis extend only down to 27.5 Å

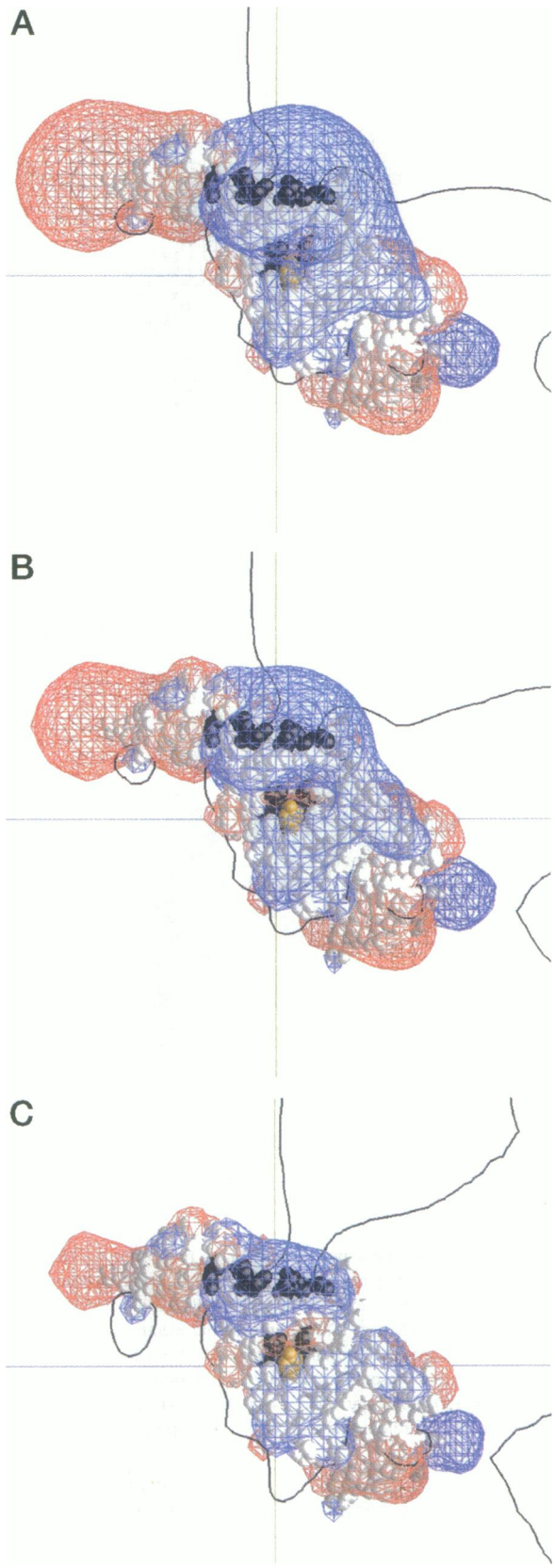

FIGURE 3 Electrostatic potential field of reduced cyt *f* for ionic strengths of (*A*) 2, (*B*) 25, and (*C*) 200 mM. All conditions except ionic strength are the same as for Fig. 2 *A*.

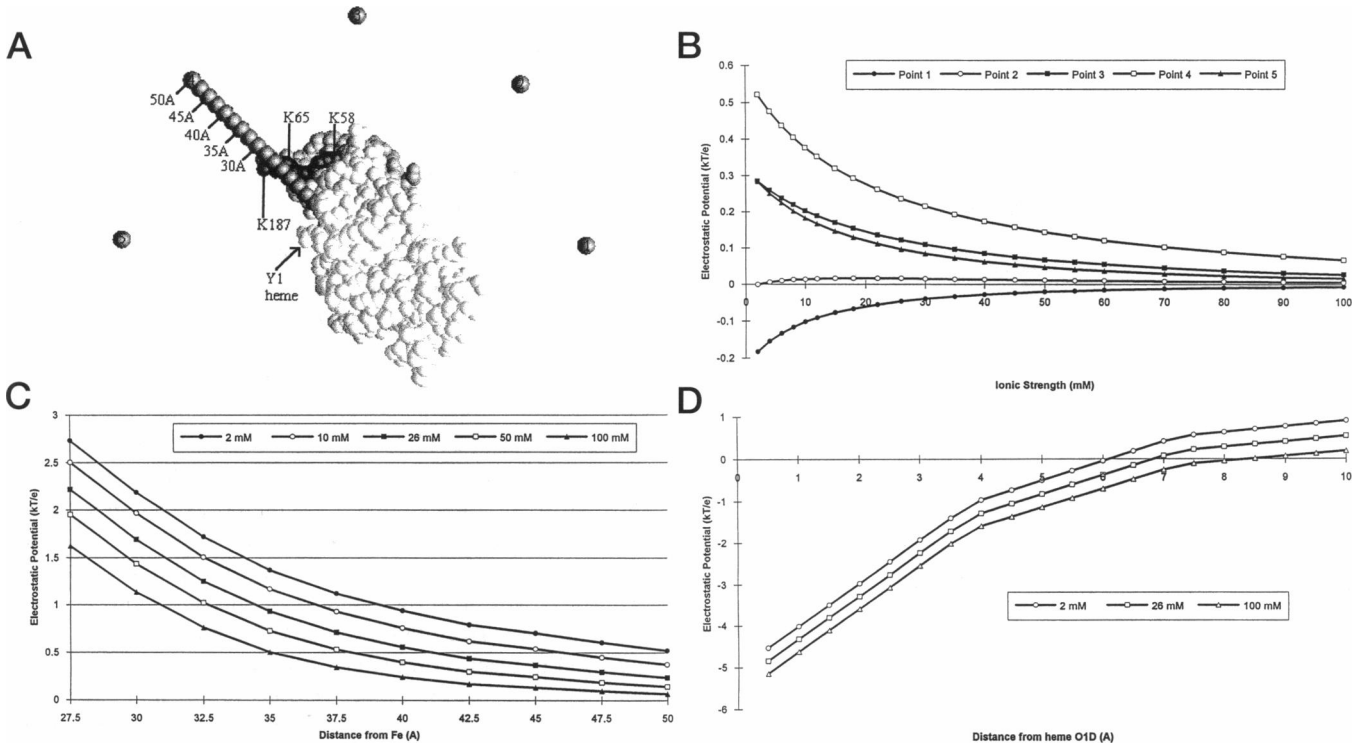

FIGURE 4 (*A*) Molecular graphic representation of points used in explicit potential calculations and relevant residues on cyt *f*. (*B*) Plot of electrostatic potential against ionic strength for points 1–5 as labeled in (*A*). Note that the greatest values are found at point 4, which is above the "positive patch" of residues 58, 65, 187, et al. (*C*) Plot of potential against distance from the heme along the axis between the heme and point 4 (as shown in *A*) for five different ionic strengths. (*D*) Plot of potential against distance from surface-exposed carboxyl on the heme for three different ionic strengths.

away from the heme because only points an appreciable distance outside the molecular surface of cyt *f* are of interest here; including points within the molecular surface would make the plot difficult to read and interpret. The molecular surface crosses the axis at a distance of 24.6 Å from the iron center.) For an ionic strength of 100 mM, a field of 0.5 kT/*e* exists up to 35 Å away from the molecular surface; this number jumps to 50 Å when ionic strength is lowered to 2 mM.

Lastly, to demonstrate that there is an increase in negative field strength around the propionic side chains of the heme as ionic strength increases, a second series of points was established extending up to 10 Å away from one of the oxygen atoms on the heme (atom O1D) with a spacing of 0.5 Å. Electrostatic potentials were mapped onto these points and plotted as a function of distance for three different ionic strengths, as shown in Fig. 4 *D*. The results plainly demonstrate an increase in the extent of the negative field as ionic strength increases, from up to 6 Å away at 2 mM to 8 Å away at 100 mM.

Comparison of oxidized and reduced states

We determined the electrostatic field of oxidized cyt *f* by using the crystal structure for reduced (Fe^{2+}) cyt *f* and changing the charge on the iron center from +2 to +3. The only effect is a small change in the positive electrostatic field in the vicinity of the heme (Fig. 5 *A*). There is little overall effect because the positive electrostatic field is dominated by the charges on positively charged amino acid side chains rather than on the heme itself.

Calculation of low-pH effects

PC and cyt *f* interact in the lumen of the chloroplast thylakoid. When the chloroplast is illuminated, hydrogen ions are transported from the stroma to the lumen, creating an acidic environment (pH ~5) within the lumen (Rottenberg and Grunwald, 1972; Pick et al., 1974) Therefore, it is important to study the interactions of PC with cyt *f* at pH 5.0.

We used the program MacroDox to calculate the pKs at pH 5 of ionizable residues on cyt *f*, which were, in turn, used to calculate the electrostatic field on cyt *f* at pH 5. A comparison of Fig. 5 *C* with Fig. 2 *A* shows that lowering the pH from 7.0 to 5.0 for cyt *f* at 100-mM ionic strength had little effect on the electrostatic potential of cyt *f*, except that the volume of space within the zero-potential contour lines was slightly larger at pH 5.0 than at pH 7.0. In particular, the region of negative potential over the region of the propionic side chains still exists at pH 5.0 because there was almost no change in the protonation state of the heme propionic acid side chains (i.e., the charge decreased from −1.0 to −0.94 and −0.985 for the A and D propionic acid side chains, respectively). However, at 2-mM ionic strength,

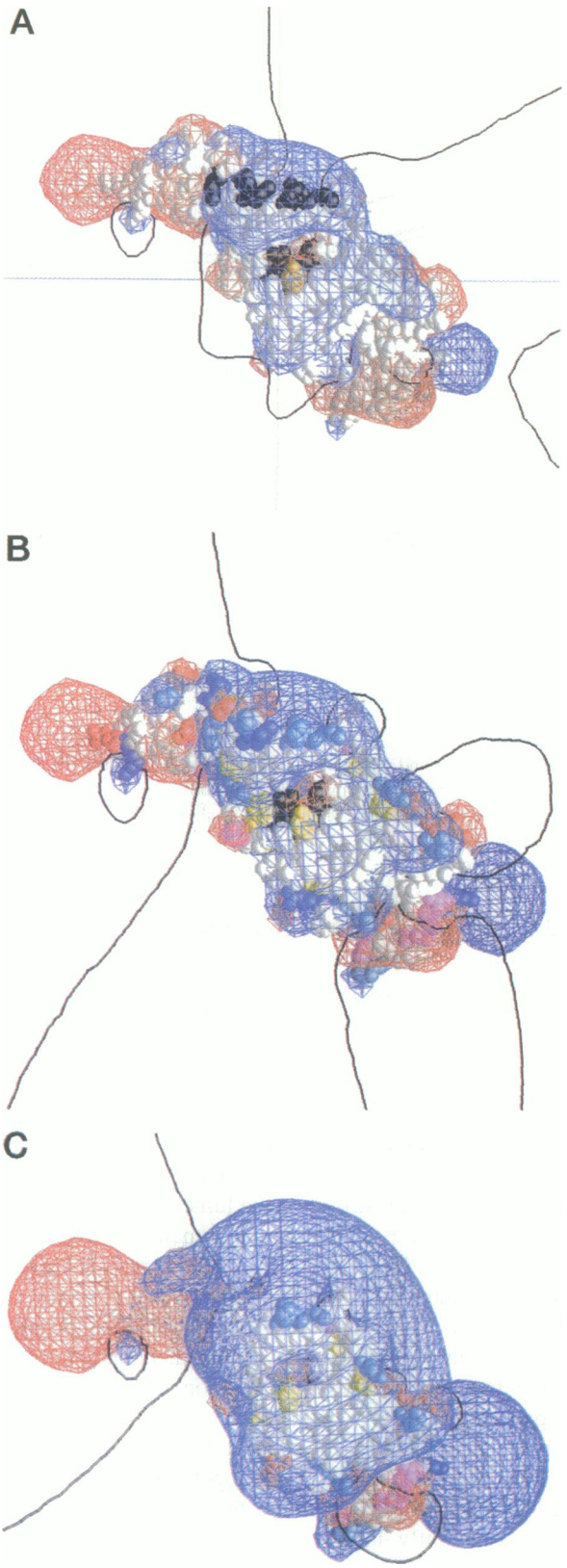

FIGURE 5 Unless otherwise noted, all conditions are the same as for Fig. 2(*A*). (*A*) Electrostatic potential field for oxidized cyt *f*. (*B*) Electrostatic potential field for reduced cyt *f* from charges calculated by Macrodox for cyt *f* at pH 5. (*C*) Electrostatic potential field for reduced cyt *f* from charges calculated by Macrodox for cyt *f* at pH 5 and 2-mM ionic strength.

a comparison of Figs. 5 *C* and 3 *A* shows that lowering the pH decreased the negative electrostatic field and increased the magnitude of the corresponding positive field.

Docked complexes

The docked complexes discussed below are based on three considerations: favorable electrostatic interactions, taken from the results calculated above and from Durell et al. (1990), possible interactions between a donor site on cyt *f* and an acceptor site on PC, and lack of steric hindrance. With respect to electron donor and acceptor sites, we assume that electron transfer can occur via either H87 or Y83 on PC (Cookson et al., 1980; Handford et al., 1980). In the case of cyt *f*, we must consider all possible electron donation sites; however, the fact that Y1 is on the surface of cyt *f* and is directly adjacent to the heme makes it one of the prime electron donor site candidates, if not *the* prime candidate. (The propionic acid side chains of the heme are also exposed to the surface but are much less likely than Y1 to be involved in electron transfer.) It is with these facts in mind that possible docking configurations of PC and cyt *f* were created with HyperChem and GRASP. Using the manual docking methods described above, we have elucidated three distinct docked complexes.

Complex 1

Complex 1 between poplar PC and turnip cyt *f* (Fig. 6 *A*) is the most electrostatically favorable complex of the three between PC and cyt *f*. When the complex is formed, the negative patch on PC is placed immediately adjacent to the positive patch of cyt *f* (not shown). However, the two proteins fit well, and there is no steric hindrance. In Fig. 6 *A* the two proteins are positioned 15 Å apart to demonstrate the electrostatic interactions that occur on approach of the two proteins. As can be seen, the amino acid side chains of both negative patches on PC are aligned with the positively charged residues on cyt *f*. In fact, this complex fits very well with the results of Morand et al. (1989) in that D44 on PC is situated next to K187 on cyt *f*; this is the pair of residues implicated in those cross-linking experiments. An examination of Complex 1 shows that E59 and E60 on PC is located next to K58 and K65 on cyt *f*. These results suggest the K58 is the unknown residue in the second cross-link identified by Morand et al. (1989) between E59 or E60 on PC and an unidentified residue on cyt *f*. Also, note the two regions of positive potential surrounding PC. One is located on the right-hand side of Fig. 6 *A*, in the regions of H87; this positive field is due to the presence of the copper ion located just below the surface of the PC molecule (Durell et al., 1990). The second positive patch is on the left-hand side in the vicinity of K54 and K77. The significance of these regions of positive potential will be discussed below. We have also obtained Complex 1 from a Brownian dynamics simulation, using the program Macrodox (Northrup et al.,

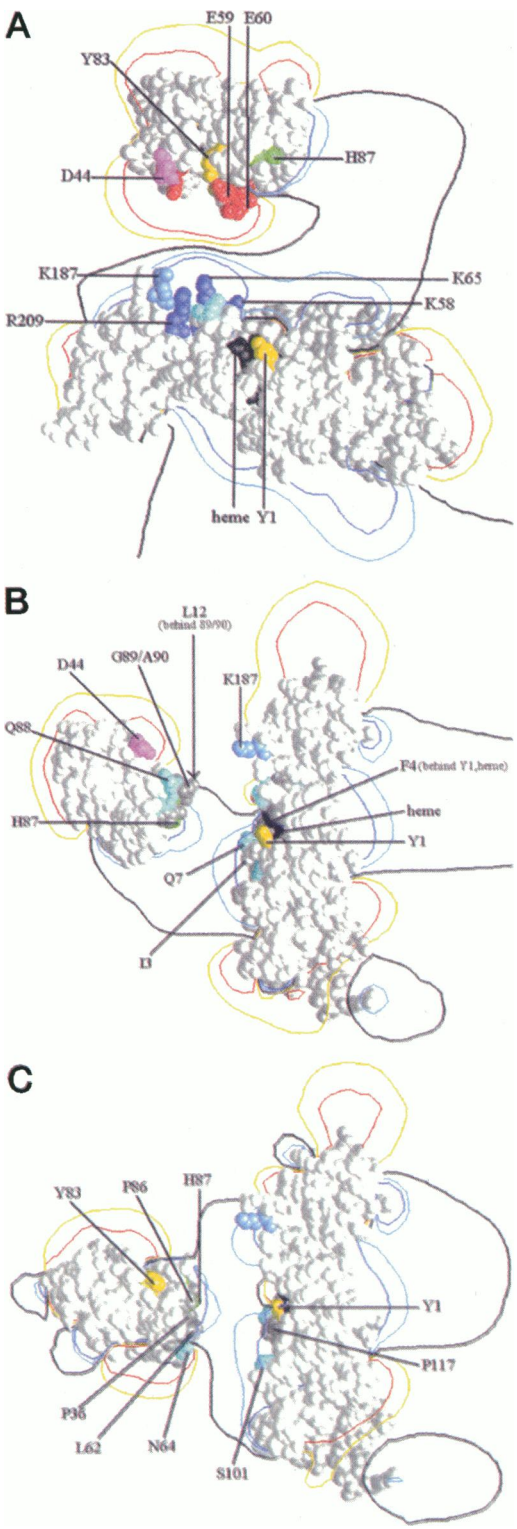

FIGURE 6 Docks of plastocyanin with cyt *f*. For all docks, plastocyanin was backed off a distance of 15 Å to show the electrostatic interactions. Ionic strength is 100 mM. Two-dimensional interpolation plane contours are colored as follows in units of kT/*e*: red, −1; yellow, −0.5; black, 0; light blue, +0.5, dark blue, +1. (*A*) Dock 1: electrostatic attraction between positive patch on cyt *f* and negative patches on PC. (*B*) Dock 2: H87 (PC)/Y1 (cyt *f*) dock with link between D44 (PC) and K187 (cyt *f*) maintained from Dock 1. (*C*) Dock 3: H87 (PC)/Y1 (cyt *f*) dock with optimization of hydrophobic interactions.

1988); the electrostatic interaction energy obtained from Macrodox for that complex was −9.8 kcal/mol (Pearson and Gross, unpublished results).

With respect to the electron transfer mechanism, there are two important questions: Which of the two sites on PC may be implicated in electron transfer, and what is the pathway from the heme on cyt *f* to that site on PC? In this complex, Y83 is closer to cyt *f* than is H87. Y83 is distant from the heme (31.4 Å) but close to the chain of water molecules that leads to the heme. The residues involved in Complex 1 are shown in Table 1.

Complex 2

Figs. 6 *B* and 7 *A* and *B* and Table 2 present a second designed complex (Complex 2). The importance of this complex is that it places H87 close to Y1 and the heme, thus providing a direct path of electron transfer from the iron atom in the heme of cyt *f* to the copper center in PC (the distance between the two metal centers is 15.6 Å). Fig. 6 *B* presents the two proteins 15 Å apart to demonstrate the electrostatic field. Fig. 7 *A* and *B* shows two views of the surfaces of the docked proteins with the areas of contact indicated.

There are four important features of this complex. First, there is the interaction between H87 on PC and Y1 on cyt *f* noted above. Second, the D44/K187 cross-link is preserved. Third, L12 is involved in this complex. Modi et al. (1992b) showed that changing this residue to an asparagine increased the interaction of PC with cyt *f*. The mutated asparagine could conceivably hydrogen bond with a tyrosine (Y1 or Y160) (or possibly the porphyrin carboxyl) in close proximity. Fourth, there are also several hydrophobic residues in the region of H87 on PC and in the region of the heme of cyt *f*. Some of these figure prominently in this complex; among them are G9, L12, and G89 on PC (as well as the β- and gamma-carbons on Q88) and F4, A62, P161 and the aromatic regions of Y1 and Y160 on cyt *f* (Table 2). Our method of estimating the interaction energy that is due to hydrophobic effects gives a covered hydrophobic surface area estimate of 256 Å^2, translating to an energy estimate of between −6.4 and −12.0 kcal/mol for this complex. The

TABLE 1 PC–Cyt *f* Complex 1

	Cyt *f*	
PC Residue	Residue	Presence in Other Complexes
E60, E61	K58	
E59, E60	N63	Complex 2
S58, E59, E60	K65	
S58, E60	K66	
E60	G67	
D44	E186	
E43, D44	K187	Complex 2
E43	R209	

TABLE 2 PC–Cyt *f* Complex 2

	Cyt *f*	
PC Residue	Residue	Presence in Other Complexes
L12, H87, P86, G89, A90	Heme	Complex 3
L12, P86, H87	Y1	Complex 3
G10, L12	F4	Complex 3
G10	Q6	
D9, G10, G11	Q7	Complex 3
D9	N8	Complex 3
G89	L61	
P86, H87, Q88, G89, A90, G91	A62	Complex 3
S85, Q88, G89	N63	Complex 1
G89	G64	
G89, A90	R156	
G89	N167	
L12, A90, G91	Y160	
D9, G10, S11	P161	
D44	K187	Complex 1

existence of hydrophobic stabilization is important because this complex does display some electrostatic repulsion, as indicated in Fig. 6 *B*, owing to the closeness of the copper atom and histidines on PC to the iron atom and associated positive charges on cyt *f*.

Also, note that there is significant overlap between PC and cyt *f* in this dock configuration, centered on G89 and A90 on PC. These residues are located on a loop with two glycines (G89, G91), which is conserved in all plastocyanins.

Complex 3

Complex 3, as shown in Figs. 6 *C* and 7 *C* and *D*, is a second H87/Y1 dock with the cross-link between D44 on PC and K187 on cyt *f* broken to allow greater interaction between hydrophobic residues on both molecules. The distance between the copper and the iron atoms is 15.3 Å. Specifically, L12, F35, P36, and L62 among others participate on PC, and I3, F4, and P117 along with the hydrocarbon chains of Q7 and Q103 participate on cyt *f* (Table 3). The electrostatic repulsion present in Complex 2 is even greater here, making the contact between hydrophobic residues even more important. We estimate the covered hydrophobic surface area in this comples to be 385 Å^2, translating to a hydrophobic interaction energy estimate of −9.6 to −18.1 kcal/mol. Some steric overlap remains in this configuration; however, the overlap is much less significant than in Complex 2.

DISCUSSION

Electrostatic field of cytochrome *f*

The most important feature of the electrostatic field of turnip cyt *f* is the positive patch of amino acid residues including K58, K65, K66, K122, K185, K187, and R209. The iron atom of the heme also contributes to this positive field, which surrounds the center of the cyt *f* molecule. We believe that the function of this positively charged field is to attract negatively charged PC into the vicinity of cyt *f*. The existence of this field confirms findings from chemical modification studies of both PC (Takabe et al., 1984, 1986; Anderson et al., 1987) and cyt *f* (Takenaka and Takabe, 1984) that negatively charged residues on PC interact with positively charged residues on cyt *f*.

All the residues of the positive patch except R209 are conserved in all the green plant and algal species whose values of cyt *f* have been sequenced to date, including spinach (Hauska et al., 1988) and turnip (Gray et al., 1994). These results confirm the importance of the positive patch in attracting negatively charged PC. Please note, however, that these residues, with the exception of K66, are not conserved in cyanobacterial species (*Agmenellum, Nostoc,* and *Synechosystis*) and there are no other positively charged residues that could reasonably substitute for these. Furthermore, the two patches of negatively charged residues are substantially absent in cyanobacterial PCs (Gross, 1996). Thus, either the electrostatic model of interactions between PC and cyt *f* does not apply to cyanobacteria or the electrostatic interactions are quite different from those for the higher plants and green algae.

It also bears noting that the most significant residue on the small domain negative patch, E200, is present only in turnip and in no other cyt *f*, which would appear to dismiss that residue from having any functional role.

Ionic strength effects

The results depicted in Figs. 2 and 3 show that the positive potential field of cyt *f* decreases with increasing ionic strength. Thus, the attraction of PC to Complex 1 will decrease as the ionic strength is raised. The attraction between PC and cyt *f* will be decreased even further at high ionic strengths because of the decrease in the negative potential field surrounding the negative patches on PC (Durell et al., 1990). These results explain the observed salt dependence of the interaction of PC with cyt *f* (Takabe et al., 1984, 1986; Takenaka and Takabe, 1984; Anderson et al. 1987) and also the observations that an electrostatic complex between the two proteins is observed only under low ionic strength conditions (Qin and Kostic, 1993).

The effects of ionic strength in the region of the heme are even more interesting (Figs. 2–4) in that PC would be attracted to a positively charged field at very low ionic strengths but repelled from a negatively charged potential field under normal physiological conditions. In other words, under normal physiological conditions PC should not be directly attracted to the heme, suggesting that neither Complex 2 nor Complex 3 could be formed as an initial docking site.

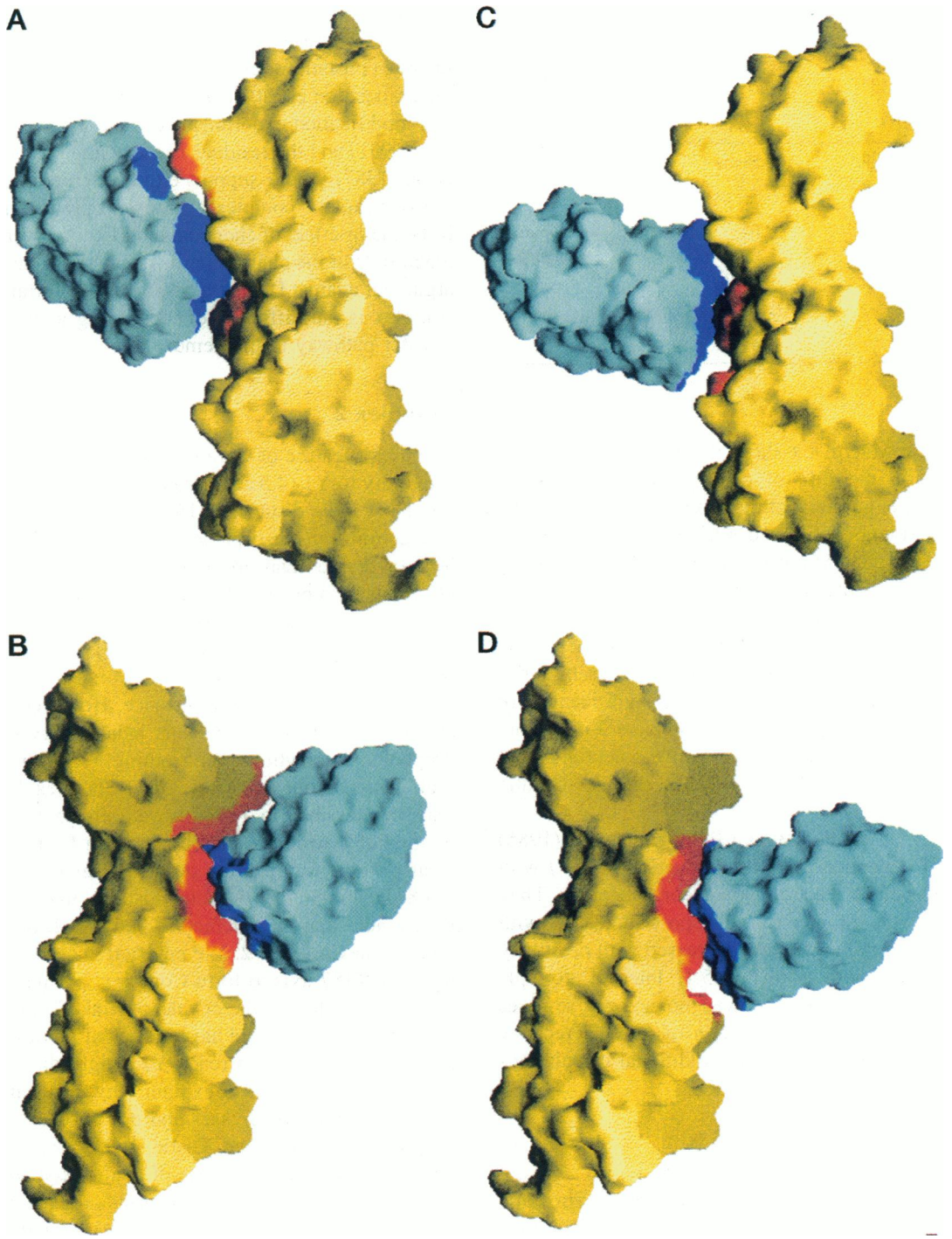

FIGURE 7 Surface representation of docks of plastocyanin with cyt *f*. In all pictures, cyt *f* is yellow with regions within 5 Å of plastocyanin colored red; PC is cyan with regions within 5 Å of cyt *f* colored dark blue. (*A*), (*B*) Two views of Dock 2. (*C*), (*D*) Two views of Dock 3.

Oxidation state effects

There is only a small effect of oxidation state on the positively charged field because the bulk of the field is contributed by the positively charged amino acid residues. These results are consistent with the observations of He et al. (1991) that changes in oxidation state have little effect on the binding of cyt *f* to PC.

pH effects

At 100-mM ionic strength, lowering the pH from 7.0 to 5.0 had little effect on the positive electrostatic field. Interestingly, there was an increase in the positive field at low pH when the ionic strength was lowered to 2 mM. These results were due to changes in the shielding of the negative charges rather than to changes in the apparent pKs of the acidic

TABLE 3 PC–Cyt *f* Complex 3

	Cyt *f*	
PC Residue	Residue	Presence in Other Complexes
P36	Heme	Complex 2
G34, P86, H87	Y1	Complex 2
G34, F35	I3	
L12, G34	F4	Complex 2
D9, G10, G34, F35	Q7	Complex 2
N64, A65	S101	
F35, N64, A65, K66	Q103	
P36	G116	
F35, L62, N64	P117	

residues because MacroDox showed a negligible effect of ionic strength on the pKs of acid groups on cyt *f*. At 100-mM ionic strength most of the observed decrease in the rate of cyt *f* oxidation observed when the pH is lowered (Beoku-Betts et al., 1985) must be due to charge effects on PC because of the small effect observed for cyt *f* shown above. This prediction is consistent with the calculations of Durell et al. (1990), who showed that lowering the pH on PC (by decreasing the charge on all acidic residues by 50%) decreased the negative electrostatic field significantly. In contrast, pH effects should be more complex at 2-mM ionic strength because the increase in the positive potential on cyt *f* opposes the corresponding decrease in the electrostatic field observed for PC.

Takabe et al. (1980) and Beoku-Betts and Sykes (1985) studied the pH dependence of the interaction of cyt *f* with low-molecular-weight electron donors or acceptors. They found that the rate of electron transport increased with negatively charged molecules and decreased with positively charged molecules with a pK of 5.1. Interestingly, pK calculations with MacroDox showed no anionic residues titrating with a pK of 5.1. Resolution of this discrepancy will require future experiments and additional calculations of pKs.

Complex 1

Complex 1 (Fig. 6 *A*) shows the most favorable electrostatic interactions of the three complexes. Because of this, it may constitute either a true electron-transfer-capable complex or a transient predocking complex. If it is the final electron-transfer-competent complex, then it must be able to carry out electron transfer, which means that an electron donation site on cyt *f* must be adjacent to an electron acceptor site on PC. In Complex 1, neither the heme nor its ligands can be electron donors because they are too distant from PC. The only possible electron transfer pathway is the chain of water molecules extending from the heme to the vicinity of K66 (Martinez et al., 1995b). With respect to PC, Y83 is in a much more favorable position for electron transfer than is H87. The function of Y83 as an electron acceptor agrees with the site-directed mutagenesis studies (He et al., 1991) of Y83, which showed that mutating this residue decreased the rate constant for electron transfer (k_{et}) as well as altering the association constant (K_a). On the other hand, the chemical modification experiments of both Y83 (Gross and Curtiss., 1991) and the residues in the acidic patches (Anderson et al., 1987) would support either interpretation (electron-transfer-capable complex or transient predocking complex) if the major effect of chemical modification were to alter the magnitude of the charges in the negative patches. The major argument against Dock 1 as a true electron-transfer-capable complex is the difficulty of identifying a suitable electron transfer pathway to the heme.

Complex 2

The major feature of Complex 2 (Fig. 6 *B*) is that H87 is in proximity to Y1 (4.5 Å), permitting efficient electron transfer. The Cu–Fe distance is 15.6 Å. Thus, it could qualify as an electron-transfer-capable complex. The electrostatics are less favorable than for Complex 1 (i.e., there is some electrostatic repulsion between positively charged groups on cyt *f* and the positive electrostatic field surrounding H87). Thus, this complex would not be favored as an initial predocking complex because PC would not be attracted to form this complex from a distance. However, the unfavorable electrostatics is more than balanced by favorable hydrophobic interactions contributing −6.4 to −12.0 kcal/mol, based on our estimates. Once Complex 1 is formed, it may be possible to remove water from the surfaces of hydrophobic residues, thereby forming Complex 2. This is clearly within the realm of possibility given our estimate of −9.8 kcal/mol for the electrostatic interaction energy. Please note that the interaction between D44 and K187 is retained in Complex 2. We envisage that PC rotates about the D44-K187 axis to form Complex 2. Thus, the question arises as to whether the covalently linked complex of Morand et al. (1989) would have sufficient flexibility for PC to turn so that H87 could reach Y1. Slight differences in the cross-linkage could also explain why electron-transfer activity is seen in some cases and not in others (Takabe and Ishikawa, 1989; Qin and Kostic, 1993; D. J. Davis, unpublished results). Another piece of evidence supporting Complex 2 is the mutagenesis experiments of Modi et al. (1992a), which implicate L12 on PC in the docking with cyt *f*.

Unlike Complex 1, Complex 2 does show some steric hindrance, particularly between G89 and A90 on PC and the residues that they interact with on cyt *f*. However, slight motions in the PC molecule could decrease these. With respect to this, G89 and A90 are part of a loop that has two conserved glycines (G89 and G91), which could provide for a high degree of flexibility and a high B factor.

Complex 3

Complex 3 (Fig. 6 *C*) shares many features with Complex 2 in that H87 interacts with Y1 and the complex is stabilized

by hydrophobic interactions. To move from Complex 2 to Complex 3, PC rotates so that the number of hydrophobic residues involved in the formation of the complex is increased, as indicated by the increase of hydrophobic surface area (from 256 to 385 $Å^2$) and, accordingly, by the more favorable interaction energy (−9.6 to −18.1 kcal/mol). This breaks the D44-K187 link. We postulate that PC may move from Complex 2 to Complex 3 before electron transfer.

The electrostatics in Complex 3 are far from optimal. This may be very important because, unlike in other protein–protein interaction systems such as antigen–antibody, tight binding is not desired inasmuch as, once the reaction has occurred, PC must leave and deliver its electron to P700 in Photosystem I.

The distinction made here between Complex 2 and Complex 3 may be meaningless as far as electron transfer is concerned, because the sole issue is whether H87 on PC and Y1 on cyt *f* (assuming that H87 to Y1 is the electron-transfer pathway) are in optimal positions for electron transfer. This position may be achieved in Complex 2, or in Complex 3, or in a hybrid of the two. Because hydrophobic interactions are dependent on the hydrophobic nature of the partners and not on their identity, and because there are several different hydrophobic residues in the regions surrounding H87 on PC and the Y1/heme area on cyt *f*, several slightly different orientations of PC where H87 and Y1 are docked are quite conceivable; indeed, there may be several variations on Complexes 2 and 3 that may be electron-transfer competent.

Other docked complexes

We do not report here a manual docked complex implicating Y83 on PC in electron transfer with cyt *f* via Y1, as supported by the evidence that Y83 (He et al., 1991) participates not only in binding of PC but also in electron transfer. It is not possible to form this complex for poplar PC because of steric hindrance. In poplar PC, Y83 is surrounded (and, in the structure as identified by x-ray crystallography, buried) by the negative patches that protrude from the molecular surface, preventing access of Y83 to H87. This does not occur in parsley PC, for example, because of the deletion of residues 57 and 58 and substitution of alanine for glutamine at position 88. However, the possibility does exist that molecular motions of the side chains would permit them to bend out of the way to allow such a complex to form for poplar PC.

This, along with the observation of the loop at residues 88–91 causing steric hinderance in H87/Y1 complexes, raises the question of conformational changes in general. The dynamics of both proteins, including movement of the side chains, may permit a closer fit for any of the three complexes or for a Y83/Y1 complex. However, the question arises concerning large amplitude conformational changes that might occur on docking. In the case of PC, comparison of solution structures for PC with the crystal structures suggest that the general structure of PC is the same in solution as in the crystal and that only minor changes occur as a function of oxidation state or pH, except in the vicinity of the copper center (Gross, 1996; Freeman, 1981). At the moment, the same can not be said for cyt *f*. Any conformational changes that might occur would affect the complexes formed.

CONCLUSIONS

Cyt *f* has a large positive electrostatic potential field that is due to positively charged residues (K58, K65, K66, K187, others) and the iron of the heme. This positive field attracts negatively charged PC. Three possible complexes have been created. The most likely mechanism is the formation of an electrostatically favorable predocking complex at the site of Complex 1 followed by rearrangement to form Complex 2 before electron transfer. Rearrangement to Complex 3 is also possible. The possibility also exists that electron transfer occurs from PC in Complex 1 to a distal site on cyt *f*. Further experiments are necessary to distinguish among these possibilities.

First and foremost, thanks need to be extended to the Computational Biology Facility of the College of Biological Sciences at the Ohio State University for providing the resources necessary for us to carry out this research. We especially thank William Ray and David Stutes for their outstanding system administration and technical expertise.

We appreciate the assistance of William A. Cramer and his collaborators at Purdue University, especially Sergio Martinez, in providing the refined cyt *f* structure.

We also would like to thank Anthony Nicholls of Columbia University, the author of GRASP, and Scott Northrup of Tennessee Technological University, who wrote Macrodox. Both provided assistance and information regarding their respective software packages that went far above and beyond the call of duty, and the help of both is greatly appreciated.

Portions of this paper parallel material in: D. C. Pearson, Jr., and E. L. Gross. 1995. The docking of cytochrome *f* with plastocyanin: three possible complexes, *In* Photosynthesis: From Light to Biosphere, Vol. II. P. Mathis, editor. Kluwer Academic Publishers, Dordrecht, The Netherlands. 729–732.

REFERENCES

Anderson, G. P., D. G. Sanderson, C. H. Lee, S. Durell, L. B. Anderson, and E. L. Gross. 1987. The effect of ethylenediamine chemical modification of plastocyanin on the rate of cytochrome *f* oxidation and P700 reduction. *Biochim. Biophys. Acta.* 894:386–396.

Bagby, S., P. C. Discoll, T. S. Harvey, and H. A. O. Hill. 1994. High-resolution solution structure of reduced parsley plastocyanin. *Biochemistry.* 33:6611–6622.

Beoku-Betts, D., S. K. Chapman, C. V. Knox, and A. G. Sykes. 1985. Kinetic studies on 1:1 electron-transfer reactions involving blue copper proteins. 11. Effects of pH, competitive inhibition, and chromium (III) modification on the reaction of plastocyanin with cytochrome *f*. *Inorg. Chem.* 24:1677–1681.

Bernstein, F. C., T. F. Koetzle, G. J. B. Williams, E. F. Meyer, M. D. Brice, J. R. Rogers, O. Kennard, T. Shimanouchi, and M. Tatsumi. 1977. The Protein Data Bank: a computer-based archival file for macromolecular structures. *J. Mol. Biol.* 112:535–542.

Cookson, D. J., M. T. Hayes, and P. E. Wright. 1980. NMR studies of the interaction of plastocyanin with chromium (III) analogues of inorganic electron transfer reagents. *Biochim. Biophys. Acta.* 591:162–176.

Davis, M. E., J. D. Madura, J. Sines, B. A. Luty, S. A. Allison, and J. A. McCammon. 1991. Diffusion-controlled enzymatic reactions. *Methods Enzymol.* 202:473–496.

Durell, S. R., J. K. Labanowski, and E. L. Gross. 1990. Modeling the electrostatic potential of plastocyanin. *Arch. Biochem. Biophys.* 277: 241–254.

Freeman, H. C. 1981. Electron transfer in "blue" copper proteins. *Coord. Chem.* 21:29–52.

Gray, J. C., R. J. Rochford, and L. C. Packman. 1994. Proteolytic removal of the C-terminal transmembrane region of cytochrome *f* during extraction from turnip and charlock leaves generates a water-soluble monomeric form of the protein. *Eur. J. Biochem.* 223:481–488.

Gross, E. L. 1993. Plastocyanin: structure and function. *Photosynth. Res.* 34:359–374.

Gross, E. L. 1996. Plastocyanin: structure, location, diffusion, and electron transfer mechanisms. *In* Oxygenic Photosynthesis: The Light Reactions. D. Ort and C. Yokum, editors. Kluwer Academic Publishers, Dordrecht, The Netherlands. In press.

Gross, E. L., and A. Curtiss. 1991. The interaction of nitrotyrosine-83 plastocyanin with cytochromes *f* and *c*: pH dependence and the effect of an additional negative charge on plastocyanin. *Biochim. Biophys. Acta.* 1056:166–172.

Gross, E. L., A. Curtiss, S. R. Durell, and D. White. 1990. Chemical modification of spinach plastocyanin using 4-chloro-3,5-dinitrobenzoic acid: characterization of four singly-modified forms. *Biochim. Biophys. Acta.* 1016:107–114.

Guss, J. M., H. D. Bartunik, and H. C. Freeman. 1992. Accuracy and precision in protein crystal structure analysis: restrained least-squares refinement of the crystal structure of poplar plastocyanin at 1.33 angstroms resolution. *Acta Crystallogr. Sect. B.* 48:790–811.

Guss, J. M., and H. C. Freeman. 1983. Structure of oxidized poplar plastocyanin at 1.6 A resolution. *J. Mol. Biol.* 169:521–563.

Handford, P. M., H. A. O. Hill, R. W.-K. Lee, R. A. Henderson, and A. G. Sykes. 1980. Investigation of the binding of inorganic complexes to blue copper proteins by proton NMR spectroscopy. I. The interaction between the $[Cr(phen)3]^{3+}$ and $[Cr(CN)5]^{3+}$ ions and the Cu (I) form of parsley PC. *J. Inorg. Biochem.* 13:83–88.

Hauska, G., W. Nitschke, and R. G. Hermann. 1988. Amino acid identities in the three redox center carrying polypeptides of the cytochrome bc_1/b_6f complexes. *J. Bioenerget. Biomemb.* 20:211–228.

Harvey, S. C. 1989. Treatment of electrostatic effects in macromolecular modeling. *Proteins.* 5:72–92.

He, S., S. Modi, D. A. Bendall, and J. C. Gray. 1991. The surface-exposed residue Tyr 83 of pea plastocyanin is involved in both binding and electron transfer reactions with cytochrome *f*. *EMBO J.* 10:4011–4016.

Janin, J., and C. Chothia. 1990. The structure of protein-protein recognition sites. *J. Biol. Chem.* 265:16027–16030.

Lee, B., and F. M. Richards. 1971. The interpretation of protein structures: estimation of static accessibility. *J. Mol. Biol.* 55:379–400.

Martinez, S. E., W. A. Cramer, and J. L. Smith. 1995a. An internal water chain in cytochrome *f*. *Biophys. J.* 68:A246.

Martinez, S. E., D. Huang, A. Szczepaniak, W. A. Cramer, and J. L. Smith. 1995b. Crystal structure of the chloroplast cytochrome *f* reveals a novel cytochrome fold and unexpected heme ligation. *Structure.* 2:95–105.

Matthew, J. B. 1985. Electrostatic effects in proteins. *Ann. Rev. Biophys. Biophys. Chem.* 14:387–417.

Matthew, J. B., and F. R. N. Gurd. 1986. Calculation of electrostatic interactions in proteins. *Methods Enzymol.* 130:413–436.

Modi, S., S. He, J. C. Gray, and D. S. Bendall. 1992a. The role of surface exposed tyr-83 of plastocyanin in electron transfer from cytochrome *c*. *Biochim. Biophys. Acta.* 1101:64–68.

Modi, S., M. Nordling, L. G. Lundberg, O. Hannson, and D. S. Bendell. 1992b. Reactivity of cytochromes *c* and *f* with mutant forms of spinach plastocyanin. *Biochim. Biophys. Acta.* 1102:85–90.

Morand, L. Z., M. K. Frame, K. K. Colvert, D. A. Johnson, D. W. Krogmann, and D. J. Davis. 1989. Plastocyanin cytochrome *f* interaction. *Biochemistry.* 28:8039–8047.

Nicholls, A., and K. A. Sharp. 1989. "DelPhi documents" file within the DelPhi macromolecular electrostatics modeling package, version 3.0. Columbia University, New York, NY.

Nicholls, A., K. A. Sharp, and B. Honig. 1991. Protein folding and association: insights from the interfacial and thermodynamic properties of hydrocarbons. *Proteins.* 11:281–296.

Niwa, S., Ishikawa, H., Nikai, S., and Takabe, T. 1980. Electron transfer reactions between cytochrome *f* and plastocyanin from *Brassica komatuna*. *J. Biochem. (Tokyo)* 88:1177–1183.

Northrup, S. H. 1995. Macrodox v.2.0.2: Software for Prediction of Macromolecular Interaction. Tennessee Technological University, Cookeville, TN.

Northrup, S. H., J. O. Boles, and J. C. L. Reynolds. 1988. Brownian dynamics of cytochrome *c* and cytochrome c_6 association. *Science.* 241:67–70.

Pick, U., H. Rottenberg, and M. Avron. 1974. The dependence of photophosphorylation in chloroplasts on ΔpH and external pH. *FEBS Letters.* 48:32–36.

Qin, L., and N. M. Kostic. 1993. Importance of protein rearrangement in the electron-transfer reaction between the physiological partners cytochrome *f* and plastocyanin. *Biochemistry.* 32:6073–6080.

Richards, F. M. 1977. Areas, volumes, packing, and protein structure. *Ann. Rev. Biophys. Bioeng.* 6:151–176.

Rose, G. D, and R. H. Wolfenden. 1993. Hydrogen bonding, hydrophobicity, packing and protein folding. *Ann. Rev. Biophys. Biomol. Struct.* 22:381–415.

Rottenberg, H., and T. Grunwald. 1972. Determination of ΔpH in chloroplasts. 3. Ammonium uptake as a measure of ΔpH in chloroplasts and subchloroplast particles. *Eur. J. Biochem.* 25:71–74.

Sharp, K. A., and B. A. Honig. 1990. Electrostatic interactions in macromolecules: theory and applications. *Ann. Rev. Biophys. Biophys. Chem.* 19:301–332.

Sharp, K. A., A. Nicholls, R. F. Fink, and B. Honig. 1991. Reconciling the magnitude of microscopic and macroscopic hydrophobic effects. *Science.* 252:107–109.

Sykes, A. G. 1991. Plastocyanin and the blue copper proteins. *Struct. Bond.* 75:175–224.

Takabe, T., and H. Ishikawa. 1989. Kinetic studies on a cross-linked complex between plastocyanin and cytochrome *f*. *J. Biochem. (Tokyo).* 105:98–102.

Takabe, T., H. Ishikawa, S. Niwa, and Y. Tanaka. 1984. Electron transfer reactions of chemically-modified plastocyanins with P700 and cytochrome *f*. Importance of local charges. *J. Biochem. (Tokyo).* 96:385–393.

Takabe, T., S. Niwa, H. Ishikawa, and K. Takenaka. 1980. Electron transfer reactions of cytochrome *f* from *Brassica komatsuna* with hexacyanoferrate. *J. Biochem. (Tokyo).* 88:1167–76.

Takabe, T., K. Takenaka, H. Kawamura, and Y. Beppu. 1986. Charges on proteins and distances of electron transfer in metalloprotein redox reactions. *J. Biochem. (Tokyo).* 99:833–840.

Takenaka, K., and T. Takabe. 1984. Importance of local positive charges on cytochrome *f* for electron transport to plastocyanin and potassium ferricyanide. *J. Biochem. (Tokyo).* 96:1813–1821.

Warshel, A., and J. Aqvist. 1991. Electrostatic energy and macromolecular function. *Ann. Rev. Biophys. Biophys. Chem.* 20:267–298.

Watkins, J. A., M. A. Cusanovich, T. E. Meyer, and G. Tollin. 1994. A "parallel plate" electrostatic model for bimolecular rate constants applied to electron transfer proteins. *Protein Sci.* 3:2104–2114.

Yelle, R. B., N.-S. Park, and T. Ichiye. 1995. Molecular dynamics simulations of rubredoxin from *Clostridium pasteurianum*: changes in structure and electrostatic potential during redox reactions. *Proteins.* 22: 154–167.